

AD8628/AD8629/AD8630

FEATURES

- Lowest auto-zero amplifier noise
- Low offset voltage: 1 μV
- Input offset drift: 0.002 $\mu\text{V}/^\circ\text{C}$
- Rail-to-rail input and output swing
- 5 V single-supply operation
- High gain, CMRR, and PSRR: 120 dB
- Very low input bias current: 100 pA max
- Low supply current: 1.0 mA
- Overload recovery time: 10 μs
- No external components required

APPLICATIONS

- Automotive sensors
- Pressure and position sensors
- Strain gage amplifiers
- Medical instrumentation
- Thermocouple amplifiers
- Precision current sensing
- Photodiode amplifier

PIN CONFIGURATIONS

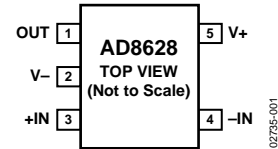


Figure 1. 5-Lead TSOT (UJ-5)
and 5-Lead SOT-23 (RT-5)

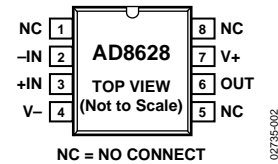


Figure 2. 8-Lead SOIC (R-8)

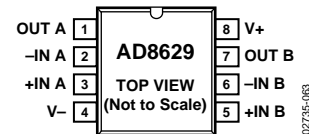


Figure 3. 8-Lead SOIC (R-8)

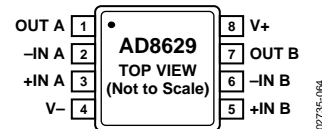


Figure 4. 8-Lead MSOP (RM-8)

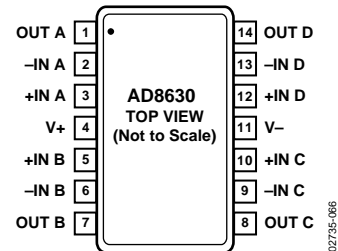


Figure 5. 14-Lead SOIC (R-14)

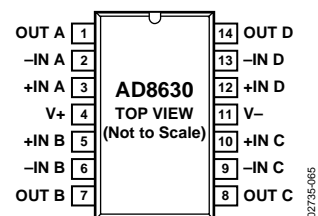


Figure 6. 14-Lead TSSOP (RU-14)

Rev. D

Information furnished by Analog Devices is believed to be accurate and reliable. However, no responsibility is assumed by Analog Devices for its use, nor for any infringements of patents or other rights of third parties that may result from its use. Specifications subject to change without notice. No license is granted by implication or otherwise under any patent or patent rights of Analog Devices. Trademarks and registered trademarks are the property of their respective owners.

TABLE OF CONTENTS

| | | | |
|---|----|---|----|
| Specifications..... | 4 | Total Integrated Input-Referred Noise for First-Order Filter | 16 |
| Electrical Characteristics – $V_s = 5.0\text{ V}$ | 4 | Input Overvoltage Protection | 17 |
| Electrical Characteristics – $V_s = 2.7\text{ V}$ | 5 | Output Phase Reversal..... | 17 |
| Absolute Maximum Ratings..... | 6 | Overload Recovery Time | 17 |
| ESD Caution..... | 6 | Infrared Sensors..... | 18 |
| Typical Performance Characteristics | 7 | Precision Current Shunt Sensor | 19 |
| Functional Description | 15 | Output Amplifier for High Precision DACs | 19 |
| 1/f Noise..... | 15 | Outline Dimensions | 20 |
| Peak-to-Peak Noise | 16 | Ordering Guide | 22 |
| Noise Behavior with First-Order Low-Pass Filter | 16 | | |

REVISION HISTORY

1/05—Rev. C to Rev. D

| | |
|---|-----------|
| Added AD8630..... | Universal |
| Added Figure 5 and Figure 6..... | 1 |
| Changes to Caption in Figure 8 and Figure 9 | 7 |
| Changes to Caption in Figure 14..... | 8 |
| Changes to Figure 17..... | 8 |
| Changes to Figure 23 and Figure 24..... | 9 |
| Changes to Figure 25 and Figure 26..... | 10 |
| Changes to Figure 31..... | 11 |
| Changes to Figure 40, Figure 41, Figure 42 | 12 |
| Changes to Figure 43 and Figure 44..... | 13 |
| Changes to Figure 51..... | 15 |
| Updated Outline Dimensions | 20 |
| Changes to Ordering Guide | 22 |

10/04—B to Rev. C

| | |
|--|-----------|
| Updated Formatting..... | Universal |
| Added AD8629..... | Universal |
| Added SOIC and MSOP Pin Configurations | 1 |
| Added Figure 48..... | 13 |
| Changes to Figure 62..... | 17 |
| Added MSOP Package | 19 |
| Changes to Ordering Guide | 22 |

10/03—Rev. A to Rev. B

| | |
|---|----|
| Changes to General Description | 1 |
| Changes to Absolute Maximum Ratings | 4 |
| Changes to Ordering Guide | 4 |
| Added TSOT-23 Package | 15 |

6/03—Rev. 0 to Rev. A

| | |
|---------------------------------------|----|
| Changes to Specifications..... | 3 |
| Changes to Ordering Guide | 4 |
| Change to Functional Description..... | 10 |
| Updated Outline Dimensions | 15 |

10/02—Revision 0: Initial Version

GENERAL DESCRIPTION

This amplifier has ultralow offset, drift, and bias current. The AD8628/AD8629/AD8630 are wide bandwidth auto-zero amplifiers featuring rail-to-rail input and output swings and low noise. Operation is fully specified from 2.7 V to 5 V single supply (± 1.35 V to ± 2.5 V dual supply).

The AD8628/AD8629/AD8630 provide benefits previously found only in expensive auto-zeroing or chopper-stabilized amplifiers. Using Analog Devices' topology, these zero-drift amplifiers combine low cost with high accuracy and low noise. No external capacitor is required. In addition, the AD8628/AD8629/AD8630 greatly reduce the digital switching noise found in most chopper-stabilized amplifiers.

With an offset voltage of only $1\ \mu\text{V}$, drift of less than $0.005\ \mu\text{V}/^\circ\text{C}$, and noise of only $0.5\ \mu\text{V}$ p-p (0 Hz to 10 Hz), the AD8628/AD8629/AD8630 are perfectly suited for applications

in which error sources cannot be tolerated. Position and pressure sensors, medical equipment, and strain gage amplifiers benefit greatly from nearly zero drift over their operating temperature range. Many systems can take advantage of the rail-to-rail input and output swings provided by the AD8628/AD8629/AD8630 to reduce input biasing complexity and maximize SNR.

The AD8628/AD8629/AD8630 are specified for the extended industrial temperature range (-40°C to $+125^\circ\text{C}$). The AD8628 is available in tiny TSOT-23, SOT-23, and the 8-lead narrow SOIC plastic packages. The AD8629 is available in the standard 8-lead narrow SOIC and MSOP plastic packages. The AD8630 quad amplifier is available in standard 14-lead SOIC and TSSOP plastic packages.

AD8628/AD8629/AD8630

SPECIFICATIONS

ELECTRICAL CHARACTERISTICS – $V_S = 5.0\text{ V}$

$V_S = 5.0\text{ V}$, $V_{CM} = 2.5\text{ V}$, $T_A = 25^\circ\text{C}$, unless otherwise noted.

Table 1.

| Parameter | Symbol | Conditions | Min | Typ | Max | Unit |
|--|--------------------------|---|----------|----------|------|------------------------------|
| INPUT CHARACTERISTICS | | | | | | |
| Offset Voltage | V_{OS} | $-40^\circ\text{C} \leq T_A \leq +125^\circ\text{C}$ | | 1 | 5 | μV |
| Input Bias Current (AD8630) | I_B | $-40^\circ\text{C} \leq T_A \leq +125^\circ\text{C}$ | | 30 | 100 | μV |
| | | | | 100 | 300 | pA |
| Input Offset Current | I_{OS} | $-40^\circ\text{C} \leq T_A \leq +125^\circ\text{C}$ | | | 1.5 | nA |
| | | | | 50 | 200 | pA |
| Input Voltage Range Common-Mode Rejection Ratio | CMRR | $V_{CM} = 0\text{ V to } 5\text{ V}$ $-40^\circ\text{C} \leq T_A \leq +125^\circ\text{C}$ | 0 | | 5 | V |
| | | | 120 | 140 | | dB |
| Large Signal Voltage Gain ¹ | A_{VO} | $R_L = 10\text{ k}\Omega$, $V_O = 0.3\text{ V to } 4.7\text{ V}$ $-40^\circ\text{C} \leq T_A \leq +125^\circ\text{C}$ | 115 | 130 | | dB |
| | | | 125 | 145 | | dB |
| Offset Voltage Drift | $\Delta V_{OS}/\Delta T$ | $-40^\circ\text{C} \leq T_A \leq +125^\circ\text{C}$ | | 0.002 | 0.02 | $\mu\text{V}/^\circ\text{C}$ |
| OUTPUT CHARACTERISTICS | | | | | | |
| Output Voltage High | V_{OH} | $R_L = 100\text{ k}\Omega$ to ground $-40^\circ\text{C} \leq T_A \leq +125^\circ\text{C}$ | 4.99 | 4.996 | | V |
| | | | 4.99 | 4.995 | | V |
| | | | 4.95 | 4.98 | | V |
| | | | 4.95 | 4.97 | | V |
| Output Voltage Low | V_{OL} | $R_L = 100\text{ k}\Omega$ to V_+ $-40^\circ\text{C} \leq T_A \leq +125^\circ\text{C}$ | | 1 | 5 | mV |
| | | | | 2 | 5 | mV |
| | | | | 10 | 20 | mV |
| | | | | 15 | 20 | mV |
| Short-Circuit Limit | I_{SC} | $-40^\circ\text{C} \leq T_A \leq +125^\circ\text{C}$ | ± 25 | ± 50 | | mA |
| | | | | ± 40 | | mA |
| Output Current | I_O | $-40^\circ\text{C} \leq T_A \leq +125^\circ\text{C}$ | | ± 30 | | mA |
| | | | | ± 15 | | mA |
| POWER SUPPLY | | | | | | |
| Power Supply Rejection Ratio | PSRR | $V_S = 2.7\text{ V to } 5.5\text{ V}$ $-40^\circ\text{C} \leq T_A \leq +125^\circ\text{C}$ | 115 | 130 | | dB |
| Supply Current/Amplifier | I_{SY} | $V_O = 0\text{ V}$ $-40^\circ\text{C} \leq T_A \leq +125^\circ\text{C}$ | | 0.85 | 1.1 | mA |
| | | | | 1.0 | 1.2 | mA |
| INPUT CAPACITANCE | | | | | | |
| Differential | C_{IN} | | | 1.5 | | pF |
| Common-Mode | | | | 8.0 | | pF |
| DYNAMIC PERFORMANCE | | | | | | |
| Slew Rate | SR | $R_L = 10\text{ k}\Omega$ | | 1.0 | | $\text{V}/\mu\text{s}$ |
| Overload Recovery Time | | | | 0.05 | | ms |
| Gain Bandwidth Product | GBP | | | 2.5 | | MHz |
| NOISE PERFORMANCE | | | | | | |
| Voltage Noise | e_n p-p | 0.1 Hz to 10 Hz | | 0.5 | | $\mu\text{V p-p}$ |
| | e_n p-p | 0.1 Hz to 1.0 Hz | | 0.16 | | $\mu\text{V p-p}$ |
| Voltage Noise Density | e_n | $f = 1\text{ kHz}$ | | 22 | | $\text{nV}/\sqrt{\text{Hz}}$ |
| Current Noise Density | i_n | $f = 10\text{ Hz}$ | | 5 | | $\text{fA}/\sqrt{\text{Hz}}$ |

¹ Gain testing is highly dependent upon test bandwidth.

ELECTRICAL CHARACTERISTICS – $V_S = 2.7\text{ V}$

$V_S = 2.7\text{ V}$, $V_{CM} = 1.35\text{ V}$, $V_O = 1.4\text{ V}$, $T_A = 25^\circ\text{C}$, unless otherwise noted.

Table 2.

| Parameter | Symbol | Conditions | Min | Typ | Max | Unit |
|--------------------------------|--------------------------|---|----------|----------|-----|------------------------------|
| INPUT CHARACTERISTICS | | | | | | |
| Offset Voltage | V_{OS} | $-40^\circ\text{C} \leq T_A \leq +125^\circ\text{C}$ | | 1 | 5 | μV |
| Input Bias Current (AD8630) | I_B | $-40^\circ\text{C} \leq T_A \leq +125^\circ\text{C}$ | | 30 | 100 | μV |
| | | | | 100 | 300 | pA |
| Input Offset Current | I_{OS} | $-40^\circ\text{C} \leq T_A \leq +125^\circ\text{C}$ | | 1.0 | 1.5 | nA |
| | | | | 50 | 200 | pA |
| Input Voltage Range | | $-40^\circ\text{C} \leq T_A \leq +125^\circ\text{C}$ | | | 250 | pA |
| Common-Mode Rejection Ratio | CMRR | $V_{CM} = 0\text{ V to } 2.7\text{ V}$ $-40^\circ\text{C} \leq T_A \leq +125^\circ\text{C}$ | 0 | | 2.7 | V |
| Large Signal Voltage Gain | A_{VO} | $R_L = 10\text{ k}\Omega$, $V_O = 0.3\text{ V to } 2.4\text{ V}$ $-40^\circ\text{C} \leq T_A \leq +125^\circ\text{C}$ | 115 | 130 | | dB |
| | | | 110 | 120 | | dB |
| Offset Voltage Drift | $\Delta V_{OS}/\Delta T$ | $-40^\circ\text{C} \leq T_A \leq +125^\circ\text{C}$ | 105 | 130 | | dB |
| OUTPUT CHARACTERISTICS | | | | | | |
| Output Voltage High | V_{OH} | $R_L = 100\text{ k}\Omega$ to ground $-40^\circ\text{C} \leq T_A \leq +125^\circ\text{C}$ | 2.68 | 2.695 | | V |
| | | | 2.68 | 2.695 | | V |
| | | | 2.67 | 2.68 | | V |
| | | | | | | V |
| Output Voltage Low | V_{OL} | $R_L = 10\text{ k}\Omega$ to ground $-40^\circ\text{C} \leq T_A \leq +125^\circ\text{C}$ | 2.67 | 2.675 | | V |
| | | | | | | V |
| | | | 1 | 5 | | mV |
| | | | | | | mV |
| Short-Circuit Limit | I_{SC} | $R_L = 100\text{ k}\Omega$ to V_+ $-40^\circ\text{C} \leq T_A \leq +125^\circ\text{C}$ | 2 | 5 | | mV |
| | | | 10 | 20 | | mV |
| | | | 15 | 20 | | mV |
| | | | ± 10 | ± 15 | | mA |
| Output Current | I_O | $-40^\circ\text{C} \leq T_A \leq +125^\circ\text{C}$ | | ± 10 | | mA |
| | | | | ± 10 | | mA |
| | | | | ± 5 | | mA |
| POWER SUPPLY | | | | | | |
| Power Supply Rejection Ratio | PSRR | $V_S = 2.7\text{ V to } 5.5\text{ V}$ $-40^\circ\text{C} \leq T_A \leq +125^\circ\text{C}$ | 115 | 130 | | dB |
| Supply Current/Amplifier | I_{SY} | $V_O = 0\text{ V}$ $-40^\circ\text{C} \leq T_A \leq +125^\circ\text{C}$ | | 0.75 | 1.0 | mA |
| | | | | 0.9 | 1.2 | mA |
| INPUT CAPACITANCE | | | | | | |
| Differential | C_{IN} | | | 1.5 | | pF |
| Common-Mode | | | | 8.0 | | pF |
| DYNAMIC PERFORMANCE | | | | | | |
| Slew Rate | SR | $R_L = 10\text{ k}\Omega$ | | 1 | | $\text{V}/\mu\text{s}$ |
| Overload Recovery Time | | | | 0.05 | | ms |
| Gain Bandwidth Product | GBP | | | 2 | | MHz |
| NOISE PERFORMANCE | | | | | | |
| Voltage Noise | e_n p-p | 0.1 Hz to 10 Hz | | 0.5 | | $\mu\text{V p-p}$ |
| Voltage Noise Density | e_n | $f = 1\text{ kHz}$ | | 22 | | $\text{nV}/\sqrt{\text{Hz}}$ |
| Current Noise Density | i_n | $f = 10\text{ Hz}$ | | 5 | | $\text{fA}/\sqrt{\text{Hz}}$ |

ABSOLUTE MAXIMUM RATINGS

Table 3.

| Parameters | Ratings |
|---|------------------------------|
| Supply Voltage | 6 V |
| Input Voltage | GND – 0.3 V to V_S + 0.3 V |
| Differential Input Voltage ¹ | ±5.0 V |
| Output Short-Circuit Duration to GND | Indefinite |
| Storage Temperature Range | |
| R, RM,RU, RT, UJ Packages | –65°C to +150°C |
| Operating Temperature Range | –40°C to +125°C |
| Junction Temperature Range | |
| R, RM,RU, RT, UJ Packages | –65°C to +150°C |
| Lead Temperature Range (Soldering, 60 sec) | 300°C |

¹ Differential input voltage is limited to ±5 V or the supply voltage, whichever is less.

Stresses above those listed under Absolute Maximum Ratings may cause permanent damage to the device. This is a stress rating only; functional operation of the device at these or any other conditions above those indicated in the operational section of this specification is not implied. Exposure to absolute maximum rating conditions for extended periods may affect device reliability.

Table 4. Thermal Characteristics

| Package Type | θ_{JA} ¹ | θ_{JC} | Unit |
|-----------------------|----------------------------|---------------|------|
| 5-Lead TSOT-23 (UJ-5) | 207 | 61 | °C/W |
| 5-Lead SOT-23 (RT-5) | 230 | 146 | °C/W |
| 8-Lead SOIC (R-8) | 158 | 43 | °C/W |
| 8-Lead MSOP (RM-8) | 190 | 44 | °C/W |
| 14-Lead SOIC (R-14) | 105 | 43 | °C/W |
| 14-Lead TSSOP (RU-14) | 148 | 23 | °C/W |

¹ θ_{JA} is specified for worst-case conditions, that is, θ_{JA} is specified for the device soldered in a circuit board for surface-mount packages. This was measured using a standard 2-layer board.

ESD CAUTION

ESD (electrostatic discharge) sensitive device. Electrostatic charges as high as 4000 V readily accumulate on the human body and test equipment and can discharge without detection. Although this product features proprietary ESD protection circuitry, permanent damage may occur on devices subjected to high energy electrostatic discharges. Therefore, proper ESD precautions are recommended to avoid performance degradation or loss of functionality.



TYPICAL PERFORMANCE CHARACTERISTICS

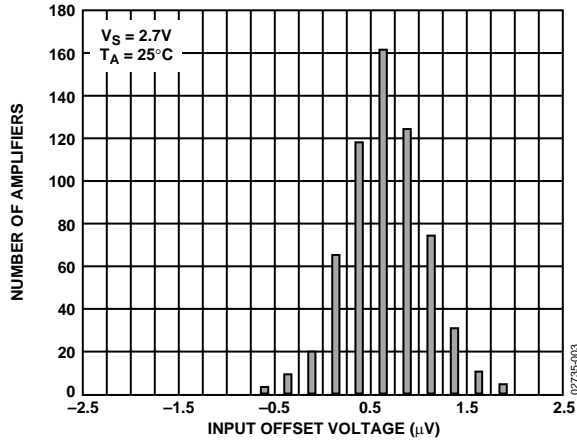


Figure 7. Input Offset Voltage Distribution at 2.7 V

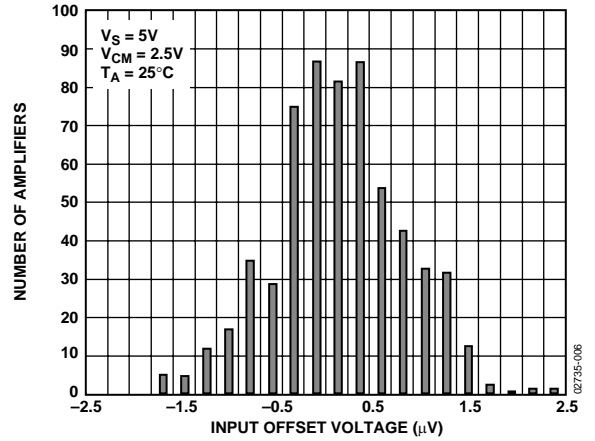


Figure 10. Input Offset Voltage Distribution at 5 V

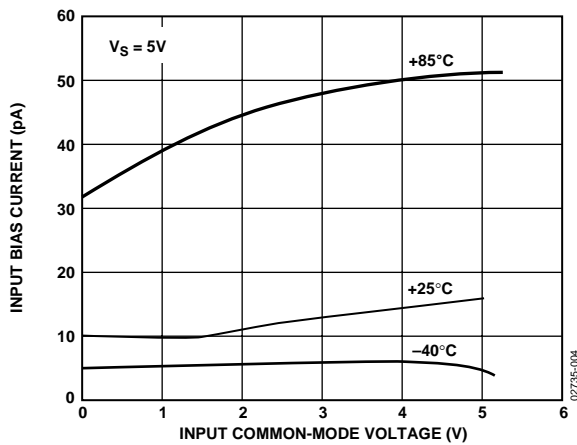


Figure 8. AD8628 Input Bias Current vs. Input Common-Mode Voltage at 5 V

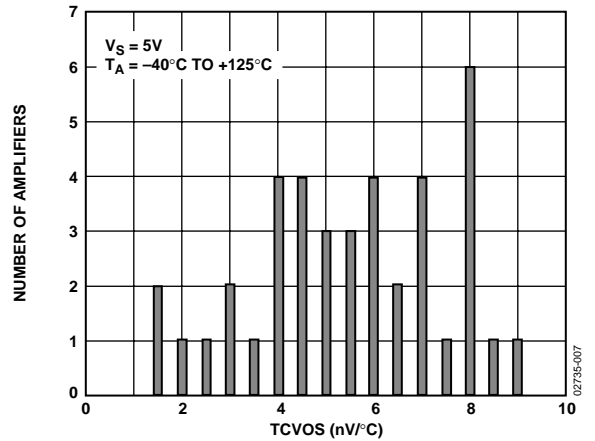


Figure 11. Input Offset Voltage Drift

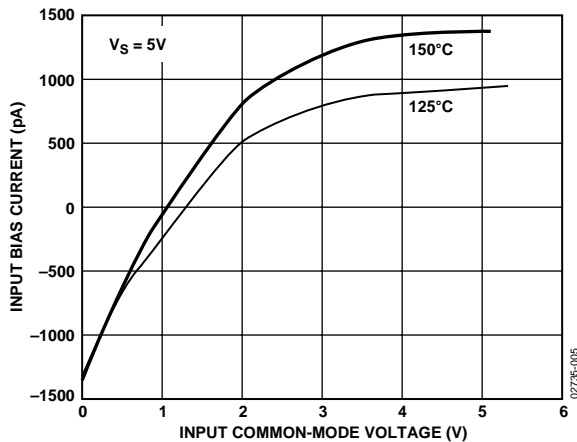


Figure 9. AD8628 Input Bias Current vs. Input Common-Mode Voltage at 5 V

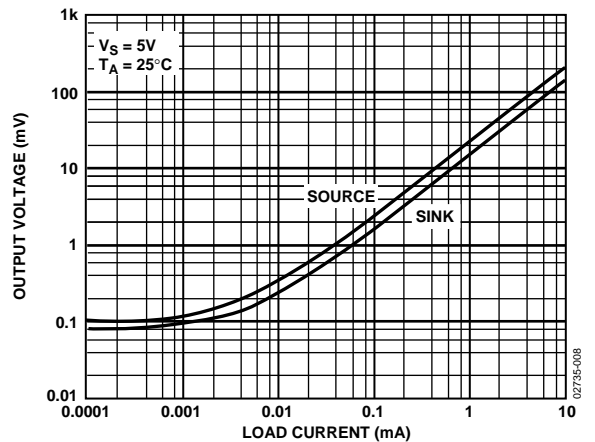


Figure 12. Output Voltage to Supply Rail vs. Load Current at 5 V

AD8628/AD8629/AD8630

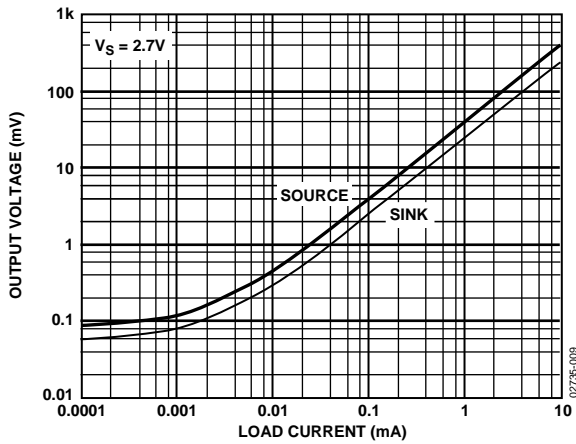


Figure 13. Output Voltage to Supply Rail vs. Load Current at 2.7V

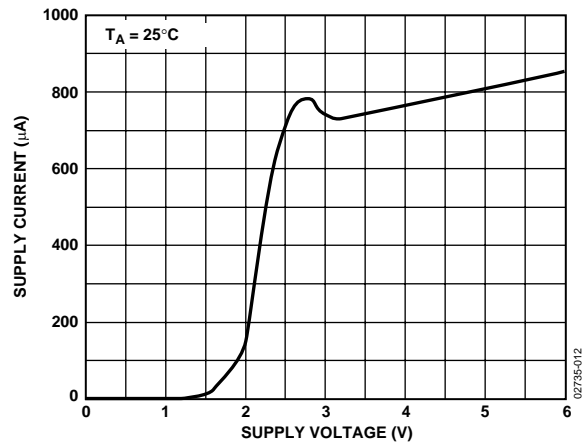


Figure 16. Supply Current vs. Supply Voltage

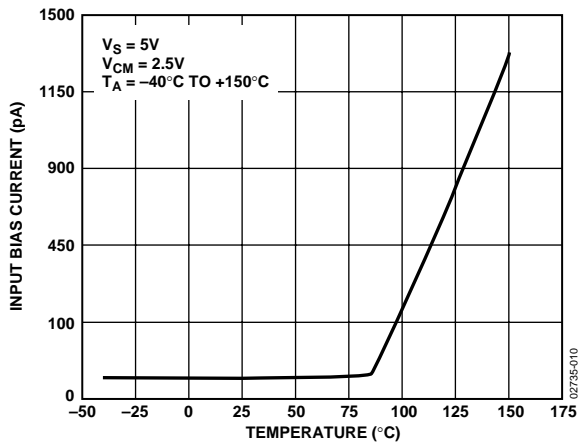


Figure 14. AD8628 Input Bias Current vs. Temperature

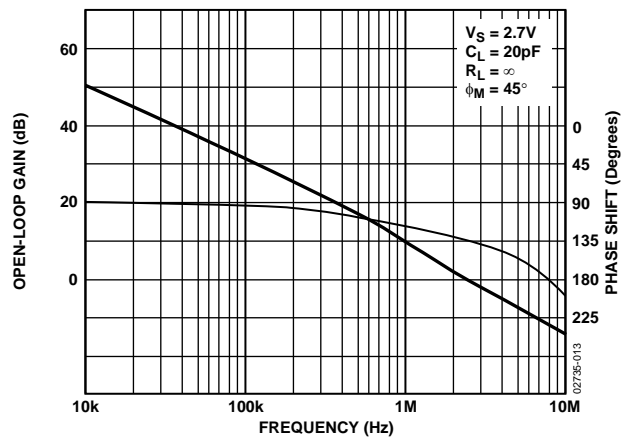


Figure 17. Open-Loop Gain and Phase vs. Frequency

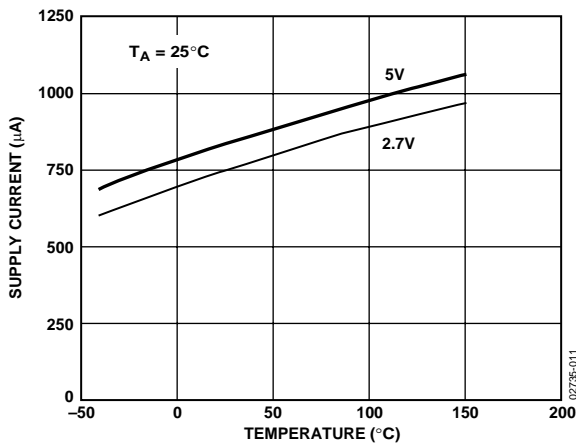


Figure 15. Supply Current vs. Temperature

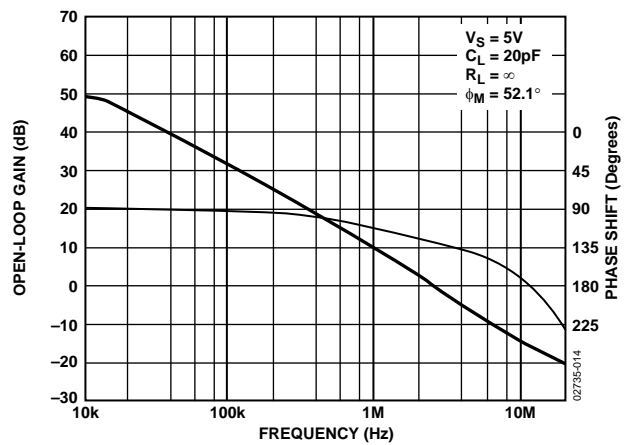


Figure 18. Open-Loop Gain and Phase vs. Frequency

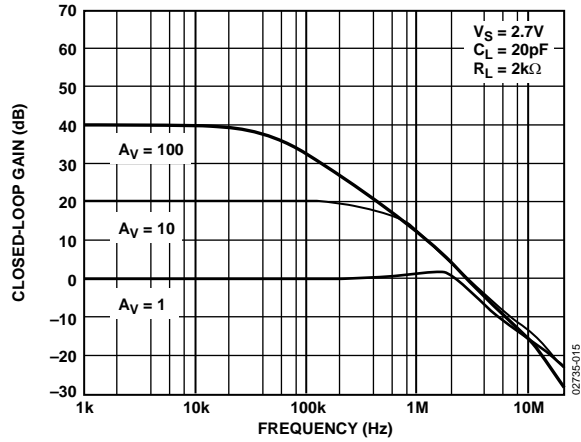


Figure 19. Closed-Loop Gain vs. Frequency at 2.7 V

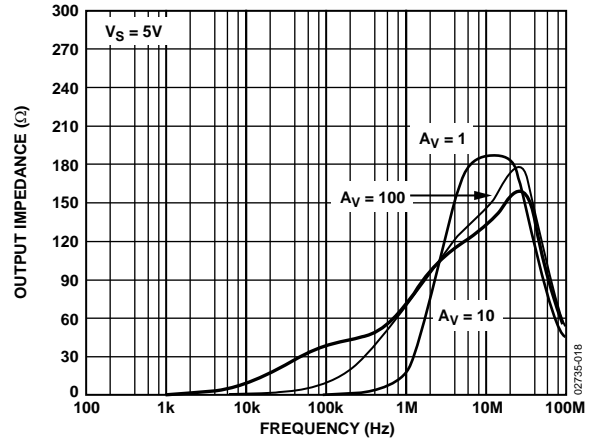


Figure 22. Output Impedance vs. Frequency at 5 V

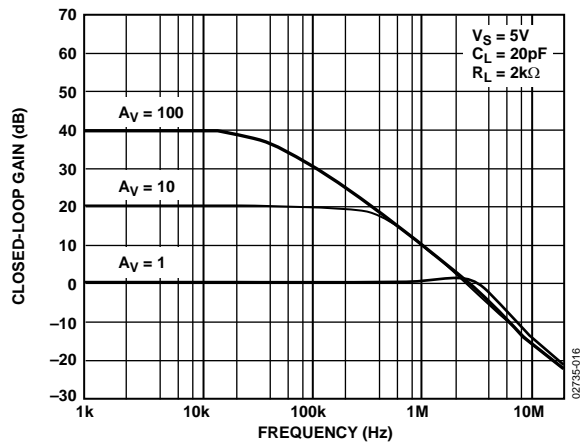


Figure 20. Closed-Loop Gain vs. Frequency at 5 V

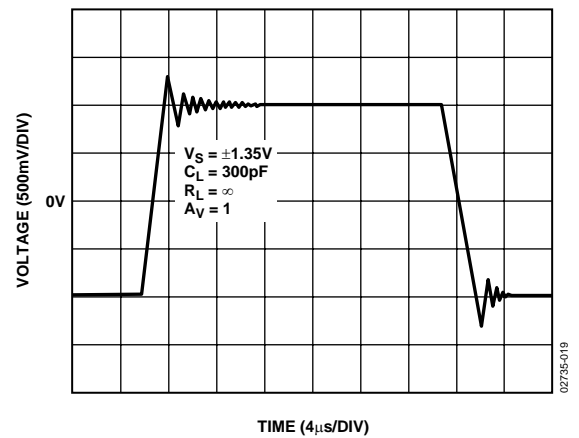


Figure 23. Large Signal Transient Response at 2.7 V

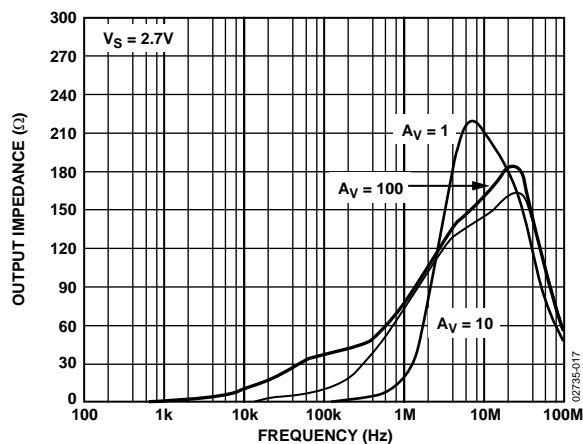


Figure 21. Output Impedance vs. Frequency at 2.7 V

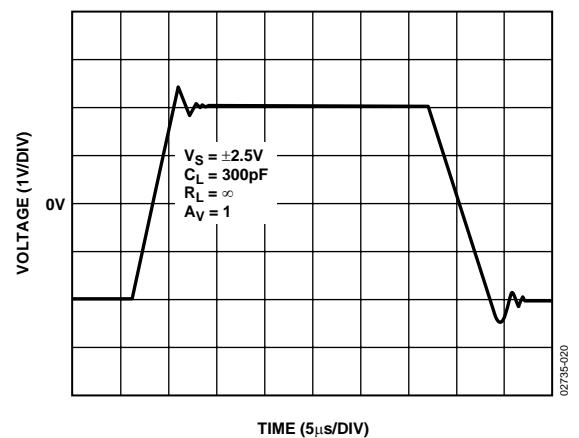


Figure 24. Large Signal Transient Response at 5 V

AD8628/AD8629/AD8630

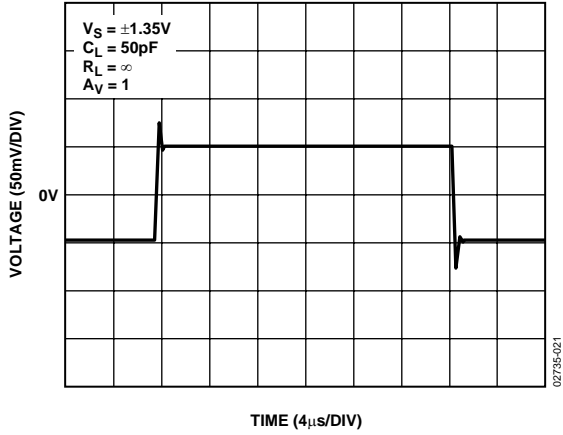


Figure 25. Small Signal Transient Response at 2.7 V

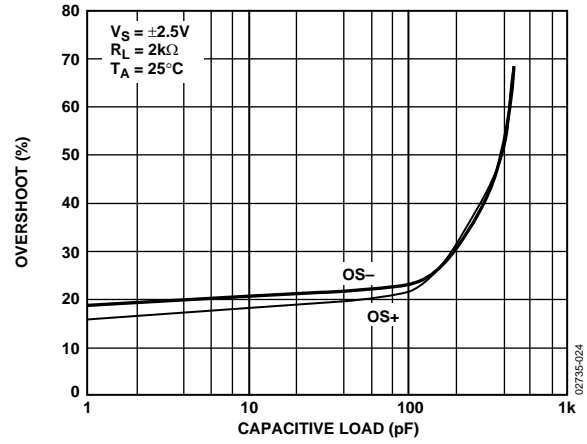


Figure 28. Small Signal Overshoot vs. Load Capacitance at 5 V

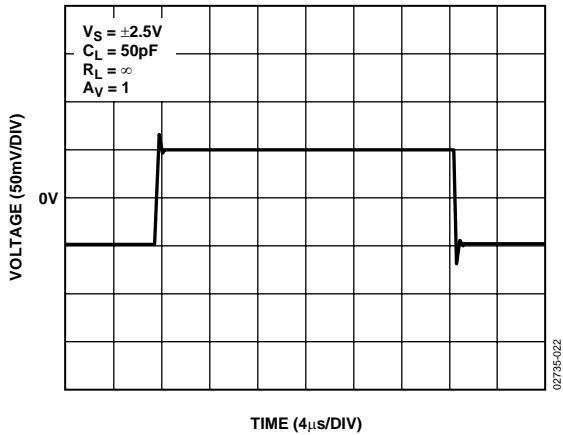


Figure 26. Small Signal Transient Response at 5 V

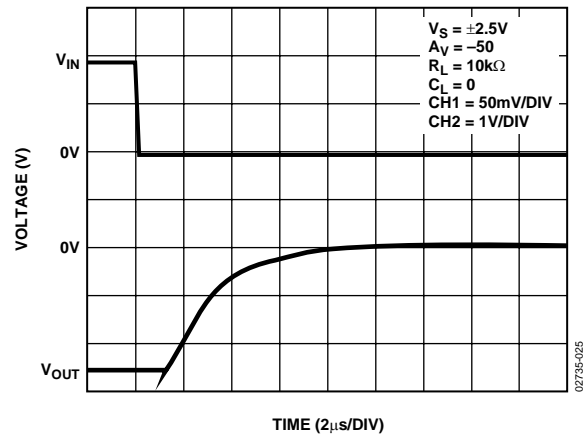


Figure 29. Positive Overtolerance Recovery

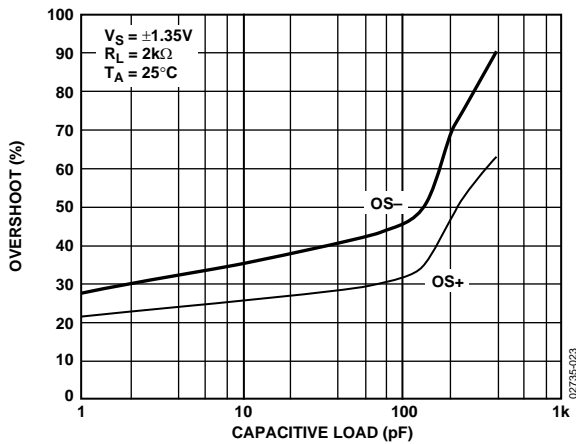


Figure 27. Small Signal Overshoot vs. Load Capacitance at 2.7 V

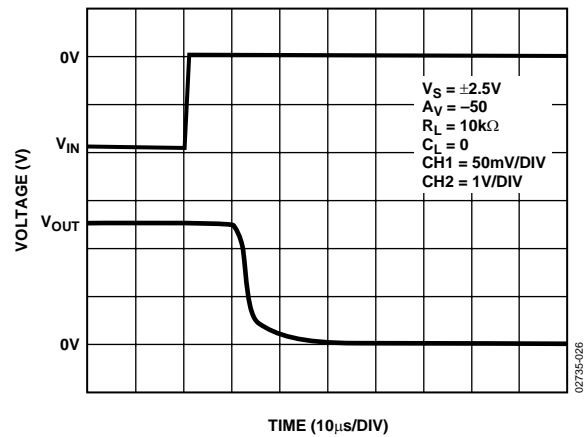


Figure 30. Negative Overtolerance Recovery

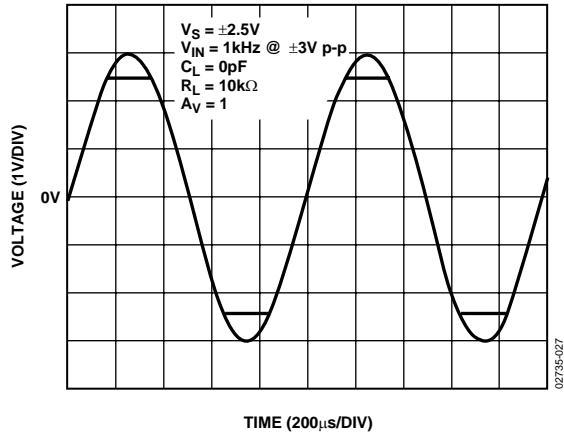


Figure 31. No Phase Reversal

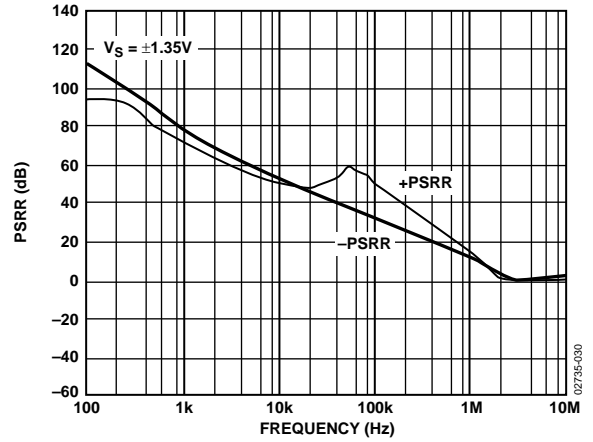


Figure 34. PSRR vs. Frequency

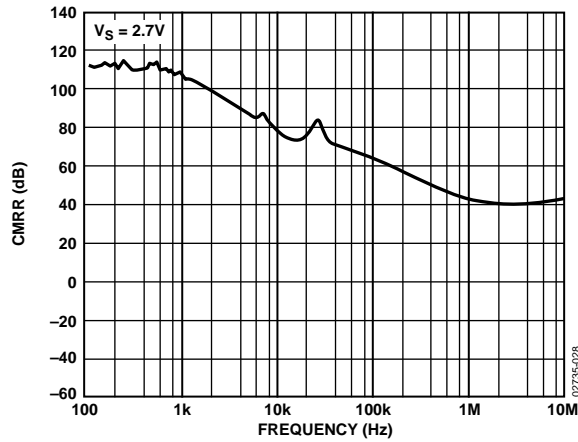


Figure 32. CMRR vs. Frequency at 2.7 V

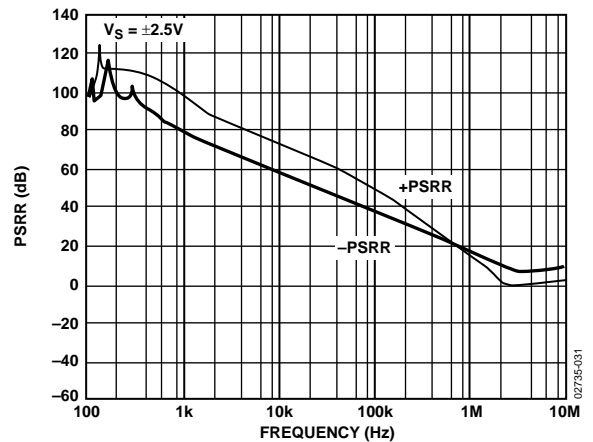


Figure 35. PSRR vs. Frequency

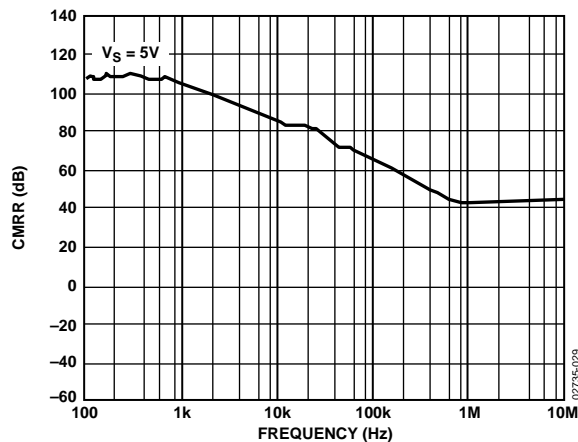


Figure 33. CMRR vs. Frequency at 5 V

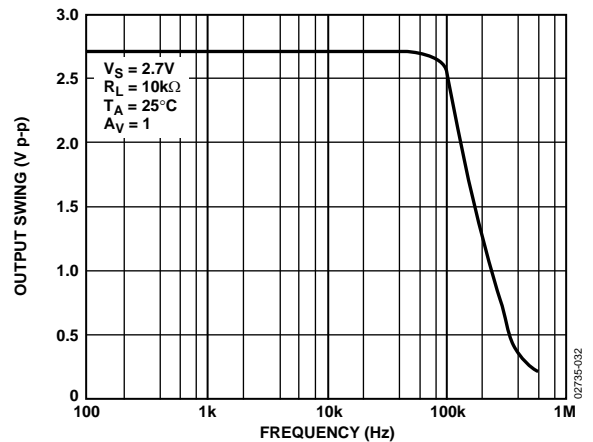


Figure 36. Maximum Output Swing vs. Frequency

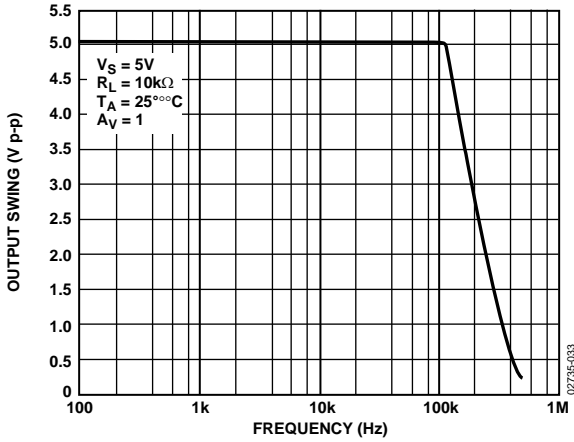


Figure 37. Maximum Output Swing vs. Frequency at 5 V

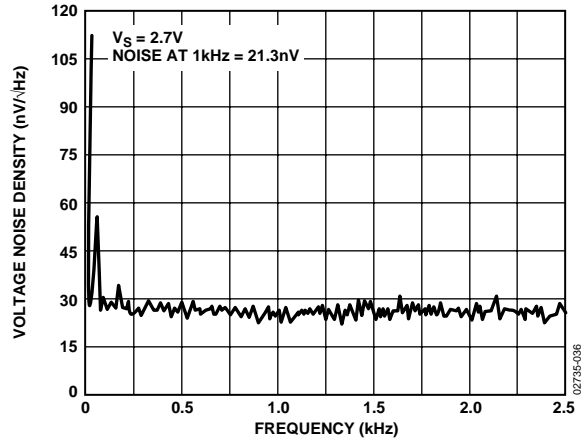


Figure 40. Voltage Noise Density at 2.7 V from 0 Hz to 2.5 kHz

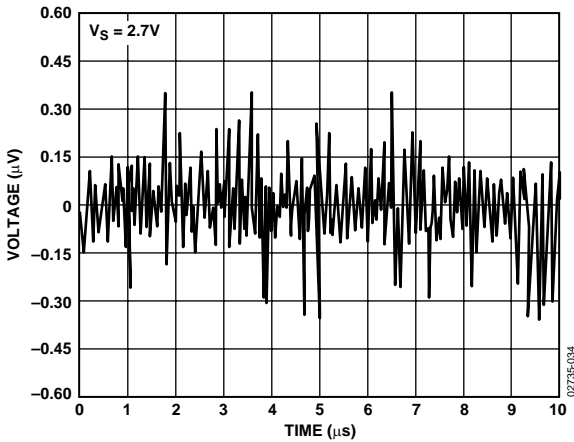


Figure 38. 0.1 Hz to 10 Hz Noise at 2.7 V

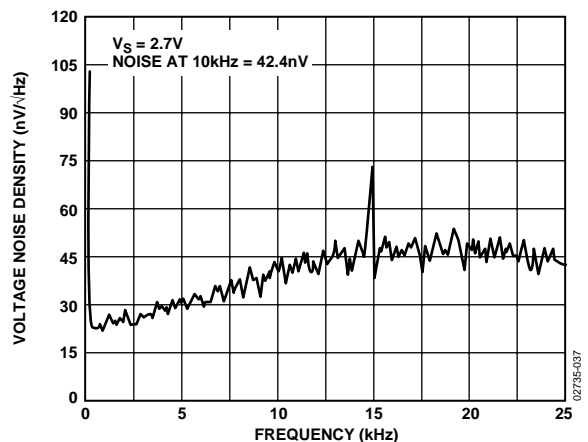


Figure 41. Voltage Noise Density at 2.7 V from 0 Hz to 25 kHz

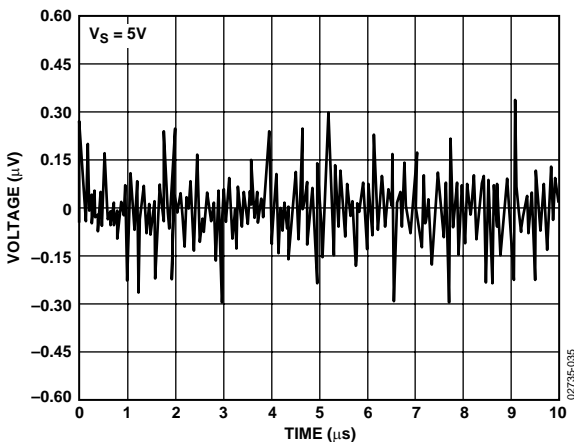


Figure 39. 0.1 Hz to 10 Hz Noise at 5 V

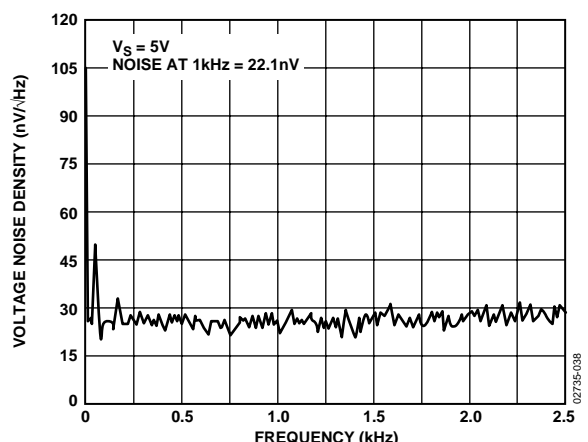


Figure 42. Voltage Noise Density at 5 V from 0 Hz to 2.5 kHz

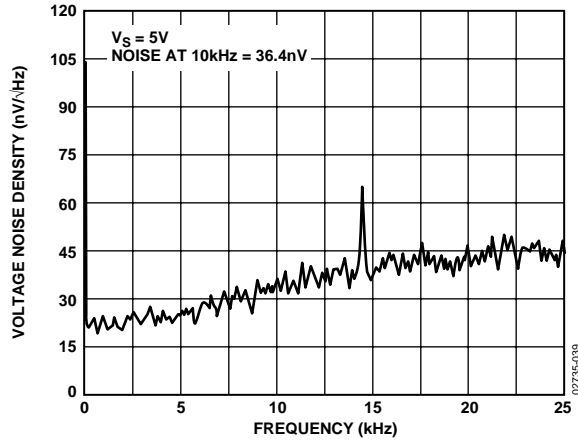


Figure 43. Voltage Noise Density at 5 V from 0 Hz to 25 kHz

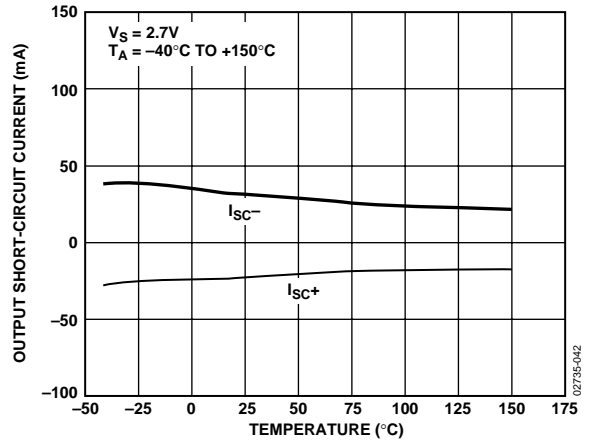


Figure 46. Output Short-Circuit Current vs. Temperature

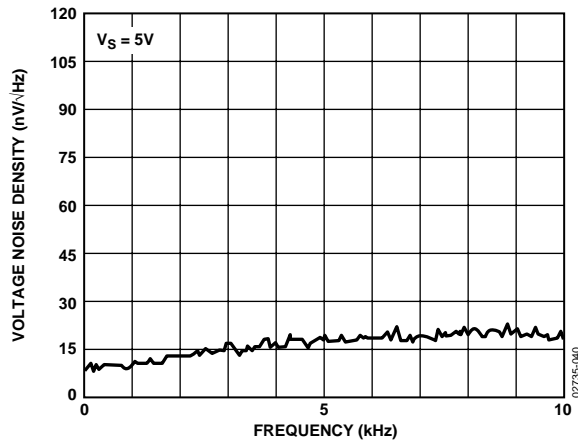


Figure 44. Voltage Noise

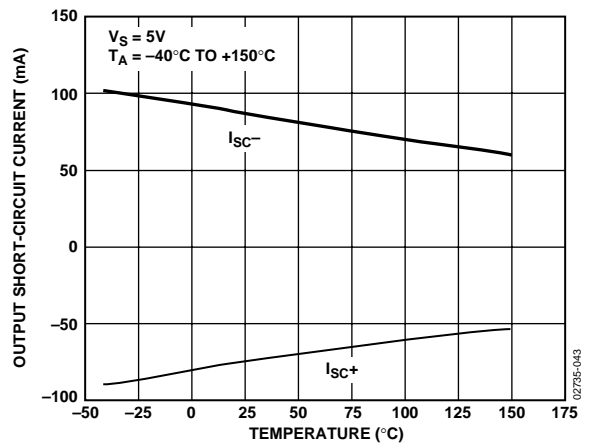


Figure 47. Output Short-Circuit Current vs. Temperature

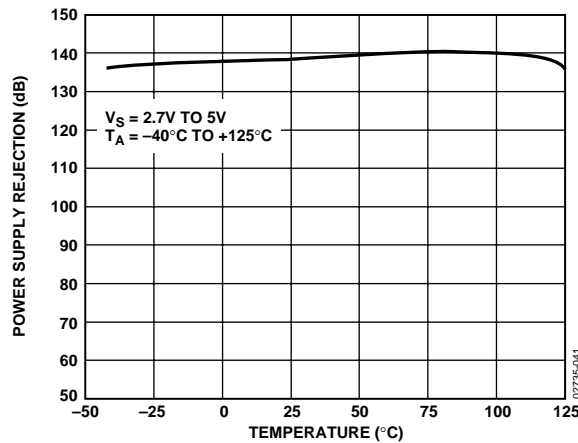


Figure 45. Power Supply Rejection vs. Temperature

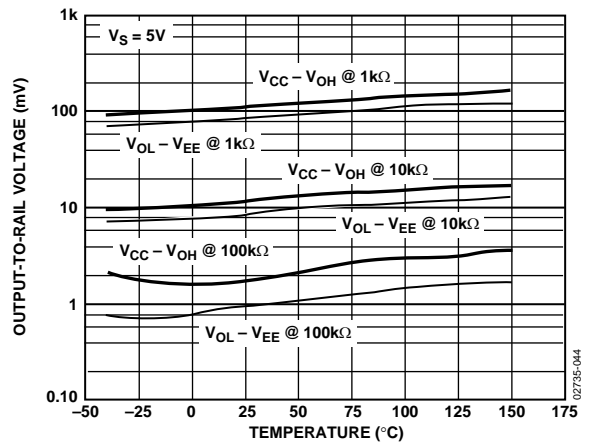


Figure 48. Output-to-Rail Voltage vs. Temperature

AD8628/AD8629/AD8630

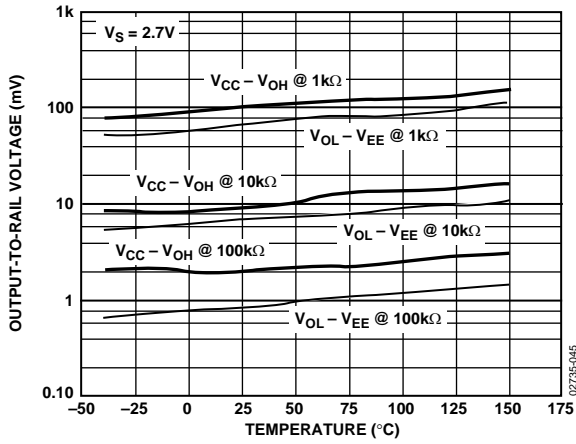


Figure 49. Output-to-Rail Voltage vs. Temperature

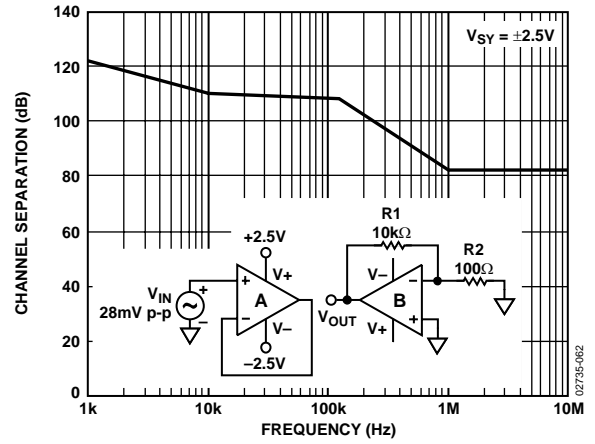


Figure 50. AD8629/AD8630 Channel Separation

FUNCTIONAL DESCRIPTION

The AD8628/AD8629/AD8630 are single-supply, ultrahigh precision rail-to-rail input and output operational amplifiers. The typical offset voltage of less than $1\ \mu\text{V}$ allows these amplifiers to be easily configured for high gains without risk of excessive output voltage errors. The extremely small temperature drift of $2\ \text{nV}/^\circ\text{C}$ ensures a minimum of offset voltage error over their entire temperature range of -40°C to $+125^\circ\text{C}$, making these amplifiers ideal for a variety of sensitive measurement applications in harsh operating environments.

The AD8628/AD8629/AD8630 achieve a high degree of precision through a patented combination of auto-zeroing and chopping. This unique topology allows the AD8628/AD8629/AD8630 to maintain their low offset voltage over a wide temperature range and over their operating lifetime. The AD8628/AD8629/AD8630 also optimize the noise and bandwidth over previous generations of auto-zero amplifiers, offering the lowest voltage noise of any auto-zero amplifier by more than 50%.

Previous designs used either auto-zeroing or chopping to add precision to the specifications of an amplifier. Auto-zeroing results in low noise energy at the auto-zeroing frequency, at the expense of higher low frequency noise due to aliasing of wide-band noise into the auto-zeroed frequency band. Chopping results in lower low frequency noise at the expense of larger noise energy at the chopping frequency. The AD8628/AD8629/AD8630 family uses both auto-zeroing and chopping in a patented ping-pong arrangement to obtain lower low frequency noise together with lower energy at the chopping and auto-zeroing frequencies, maximizing the signal-to-noise ratio (SNR) for the majority of applications without the need for additional filtering. The relatively high clock frequency of $15\ \text{kHz}$ simplifies filter requirements for a wide, useful, noise-free bandwidth.

The AD8628 is among the few auto-zero amplifiers offered in the 5-lead TSOT-23 package. This provides a significant improvement over the ac parameters of the previous auto-zero amplifiers. The AD8628/AD8629/AD8630 have low noise over a relatively wide bandwidth (0 Hz to 10 kHz) and can be used where the highest dc precision is required. In systems with signal bandwidths of from 5 kHz to 10 kHz, the AD8628/AD8629/AD8630 provide true 16-bit accuracy, making them the best choice for very high resolution systems.

1/f NOISE

1/f noise, also known as pink noise, is a major contributor to errors in dc-coupled measurements. This 1/f noise error term can be in the range of several μV or more, and, when amplified with the closed-loop gain of the circuit, can show up as a large output offset. For example, when an amplifier with a $5\ \mu\text{V}$ p-p 1/f noise is configured for a gain of 1,000, its output has 5 mV of error due to the 1/f noise. But the AD8628/AD8629/AD8630 eliminate 1/f noise internally, and thereby greatly reduce output errors.

The internal elimination of 1/f noise is accomplished as follows. 1/f noise appears as a slowly varying offset to AD8628/AD8629/AD8630 inputs. Auto-zeroing corrects any dc or low frequency offset. Therefore, the 1/f noise component is essentially removed, leaving the AD8628/AD8629/AD8630 free of 1/f noise.

One of the biggest advantages that the AD8628/AD8629/AD8630 bring to systems applications over competitive auto-zero amplifiers is their very low noise. The comparison shown in Figure 51 indicates an input-referred noise density of $19.4\ \text{nV}/\sqrt{\text{Hz}}$ at 1 kHz for the AD8628, which is much better than the LTC2050 and LMC2001. The noise is flat from dc to 1.5 kHz, slowly increasing up to 20 kHz. The lower noise at low frequency is desirable where auto-zero amplifiers are widely used.

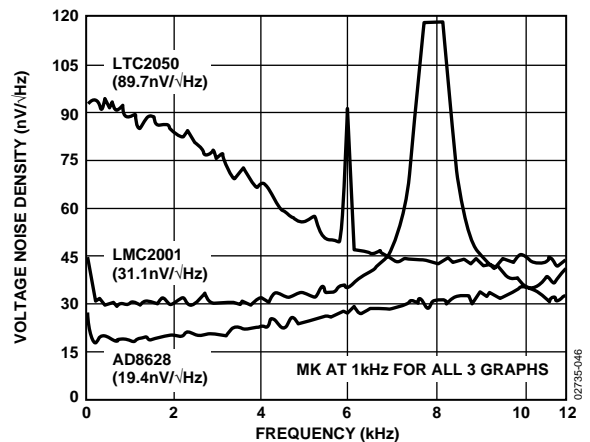


Figure 51. Noise Spectral Density of AD8628 vs. Competition

PEAK-TO-PEAK NOISE

Because of the ping-pong action between auto-zeroing and chopping, the peak-to-peak noise of the AD8628/AD8629/AD8630 is much lower than the competition. Figure 52 and Figure 53 show this comparison.

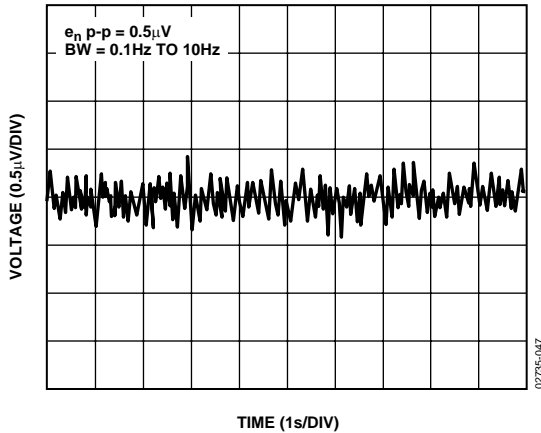


Figure 52. AD8628 Peak-to-Peak Noise

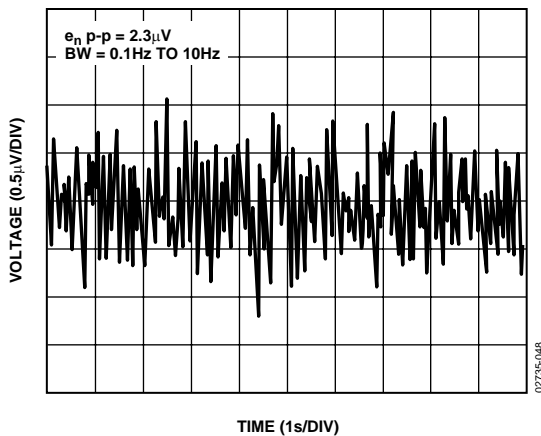


Figure 53. LTC2050 Peak-to-Peak Noise

NOISE BEHAVIOR WITH FIRST-ORDER LOW-PASS FILTER

The AD8628 was simulated as a low-pass filter (Figure 55) and then configured as shown in Figure 54. The behavior of the AD8628 matches the simulated data. It was verified that noise is rolled off by first-order filtering. Figure 55 and Figure 56 show the difference between the simulated and actual transfer functions of the circuit shown in Figure 54.

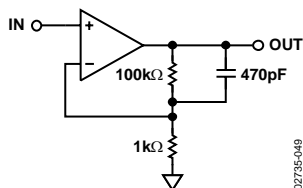


Figure 54. Test Circuit: First-Order Low-Pass Filter— $\times 101$ Gain and 3 kHz Corner Frequency

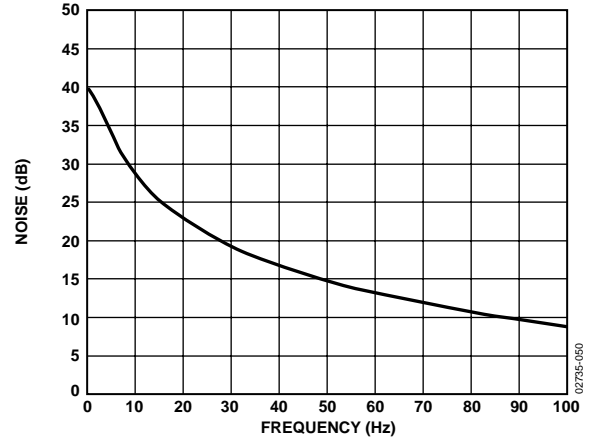


Figure 55. Simulation Transfer Function of the Test Circuit

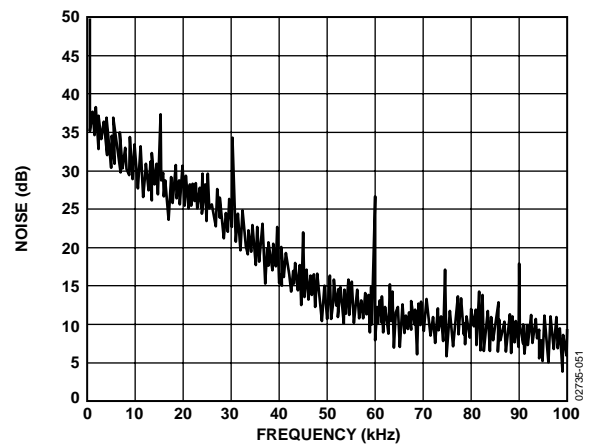


Figure 56. Actual Transfer Function of Test Circuit

The measured noise spectrum of the test circuit charted in Figure 56 shows that noise between 5 kHz and 45 kHz is successfully rolled off by the first-order filter.

TOTAL INTEGRATED INPUT-REFERRED NOISE FOR FIRST-ORDER FILTER

For a first-order filter, the total integrated noise from the AD8628 is lower than the LTC2050.

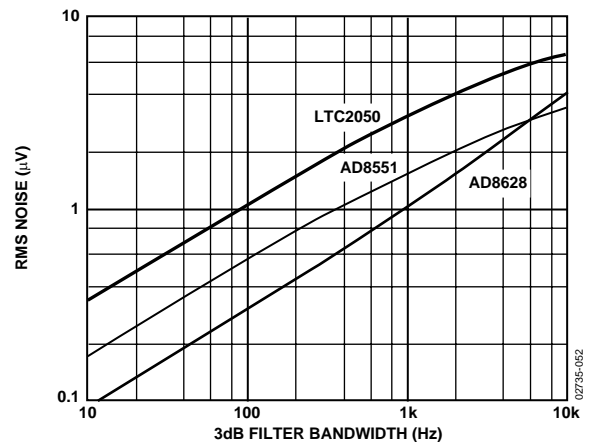


Figure 57. 3 dB Filter Bandwidth in Hz

INPUT OVERVOLTAGE PROTECTION

Although the AD8628/AD8629/AD8630 are rail-to-rail input amplifiers, care should be taken to ensure that the potential difference between the inputs does not exceed the supply voltage. Under normal negative feedback operating conditions, the amplifier corrects its output to ensure that the two inputs are at the same voltage. However, if either input exceeds either supply rail by more than 0.3 V, large currents begin to flow through the ESD protection diodes in the amplifier.

These diodes are connected between the inputs and each supply rail to protect the input transistors against an electrostatic discharge event, and they are normally reverse-biased. However, if the input voltage exceeds the supply voltage, these ESD diodes can become forward-biased. Without current limiting, excessive amounts of current could flow through these diodes, causing permanent damage to the device. If inputs are subject to overvoltage, appropriate series resistors should be inserted to limit the diode current to less than 5 mA maximum.

OUTPUT PHASE REVERSAL

Output phase reversal occurs in some amplifiers when the input common-mode voltage range is exceeded. As common-mode voltage is moved outside of the common-mode range, the outputs of these amplifiers can suddenly jump in the opposite direction to the supply rail. This is the result of the differential input pair shutting down, causing a radical shifting of internal voltages that results in the erratic output behavior.

The AD8628/AD8629/AD8630 amplifiers have been carefully designed to prevent any output phase reversal, provided that both inputs are maintained within the supply voltages. If one or both inputs could exceed either supply voltage, a resistor should be placed in series with the input to limit the current to less than 5 mA. This ensures that the output does not reverse its phase.

OVERLOAD RECOVERY TIME

Many auto-zero amplifiers are plagued by a long overload recovery time, often in ms, due to the complicated settling behavior of the internal nulling loops after saturation of the outputs. The AD8628/AD8629/AD8630 have been designed so that internal settling occurs within two clock cycles after output saturation happens. This results in a much shorter recovery time, less than 10 μ s, when compared to other auto-zero amplifiers. The wide bandwidth of the AD8628/AD8629/AD8630 enhances performance when the parts are used to drive loads that inject transients into the outputs. This is a common situation when an amplifier is used to drive the input of switched capacitor ADCs.

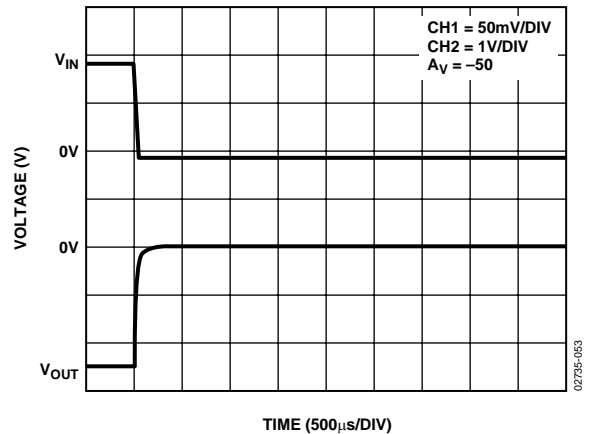


Figure 58. Positive Input Overload Recovery for the AD8628

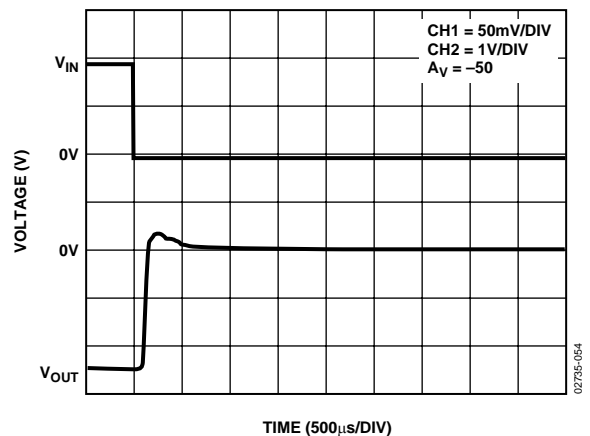


Figure 59. Positive Input Overload Recovery for LTC2050

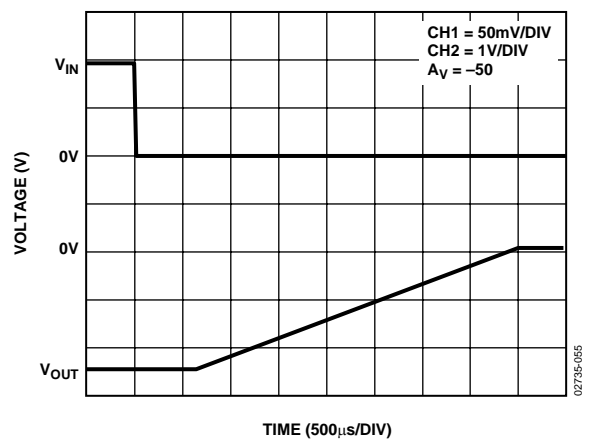


Figure 60. Positive Input Overload Recovery for LMC2001

AD8628/AD8629/AD8630

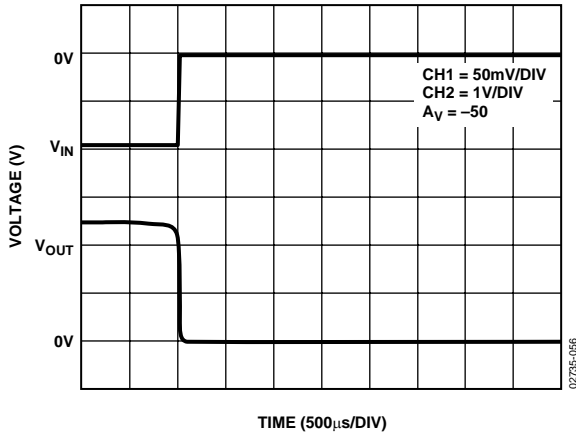


Figure 61. Negative Input Overload Recovery for the AD8628

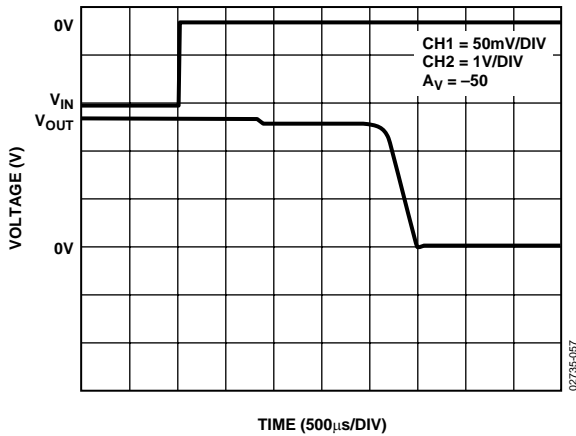


Figure 62. Negative Input Overload Recovery for LTC2050

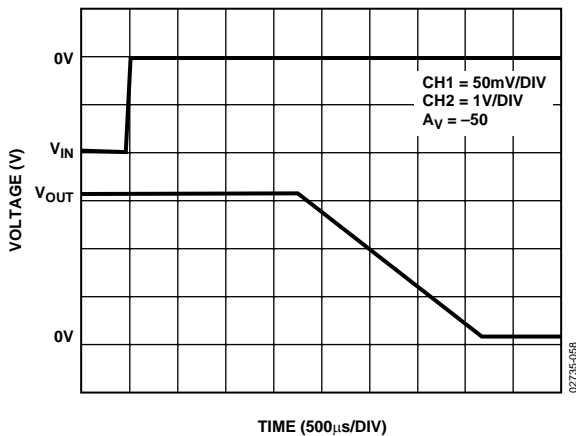


Figure 63. Negative Input Overload Recovery for LMC2001

The results shown in Figure 58 to Figure 63 are summarized in Table 5.

Table 5. Overload Recovery Time

| Product | Positive Overload Recovery (μs) | Negative Overload Recovery (μs) |
|---------|--|--|
| AD8628 | 6 | 9 |
| LTC2050 | 650 | 25,000 |
| LMC2001 | 40,000 | 35,000 |

INFRARED SENSORS

Infrared (IR) sensors, particularly thermopiles, are increasingly being used in temperature measurement for applications as wide-ranging as automotive climate control, human ear thermometers, home insulation analysis, and automotive repair diagnostics. The relatively small output signal of the sensor demands high gain with very low offset voltage and drift to avoid dc errors.

If interstage ac coupling is used, as in Figure 64, low offset and drift prevent the input amplifier's output from drifting close to saturation. The low input bias currents generate minimal errors from the sensor's output impedance. As with pressure sensors, the very low amplifier drift with time and temperature eliminate additional errors once the temperature measurement is calibrated. The low $1/f$ noise improves SNR for dc measurements taken over periods often exceeding $1/5$ s.

Figure 64 shows a circuit that can amplify ac signals from $100 \mu\text{V}$ to $300 \mu\text{V}$ up to the 1 V to 3 V level, with gain of 10,000 for accurate A/D conversion.

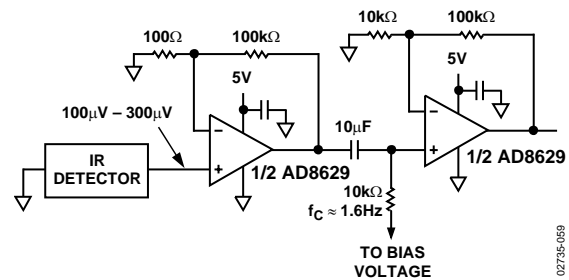


Figure 64. AD8629 Used as Preamplifier for Thermopile

PRECISION CURRENT SHUNT SENSOR

A precision current shunt sensor benefits from the unique attributes of auto-zero amplifiers when used in a differencing configuration, as shown in Figure 65. Current shunt sensors are used in precision current sources for feedback control systems. They are also used in a variety of other applications, including battery fuel gauging, laser diode power measurement and control, torque feedback controls in electric power steering, and precision power metering.

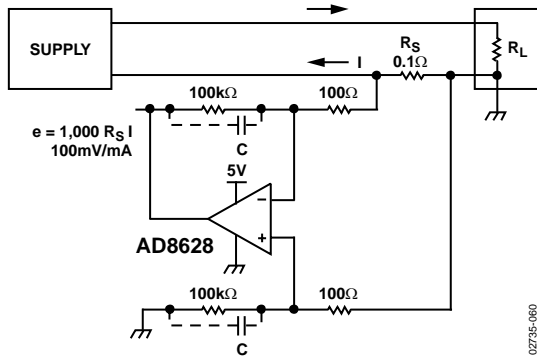


Figure 65. Low-Side Current Sensing

In such applications, it is desirable to use a shunt with very low resistance to minimize the series voltage drop; this minimizes wasted power and allows the measurement of high currents while saving power. A typical shunt might be 0.1 Ω. At measured current values of 1 A, the shunt's output signal is hundreds of mV, or even V, and amplifier error sources are not critical. However, at low measured current values in the 1 mA range, the 100 μV output voltage of the shunt demands a very low offset voltage and drift to maintain absolute accuracy. Low input bias currents are also needed, so that injected bias current does not become a significant percentage of the measured current. High open-loop gain, CMRR, and PSRR help to maintain the overall circuit accuracy. As long as the rate of change of the current is not too fast, an auto-zero amplifier can be used with excellent results.

OUTPUT AMPLIFIER FOR HIGH PRECISION DACS

The AD8628/AD8629/AD8360 are used as output amplifiers for a 16-bit high precision DAC in a unipolar configuration. In this case, the selected op amp needs to have very low offset voltage (the DAC LSB is 38 μV when operated with a 2.5 V reference) to eliminate the need for output offset trims. Input bias current (typically a few tens of picoamperes) must also be very low, because it generates an additional zero code error when multiplied by the DAC output impedance (approximately 6 kΩ).

Rail-to-rail input and output provide full-scale output with very little error. Output impedance of the DAC is constant and code-independent, but the high input impedance of the AD8628/AD8629/AD8630 minimizes gain errors. The amplifiers' wide bandwidth also serves well in this case. The amplifiers, with settling time of 1 μs, add another time constant to the system, increasing the settling time of the output. The settling time of the AD5541 is 1 μs. The combined settling time is approximately 1.4 μs, as can be derived from the following equation:

$$t_S (TOTAL) = \sqrt{(t_S DAC)^2 + (t_S AD8628)^2}$$

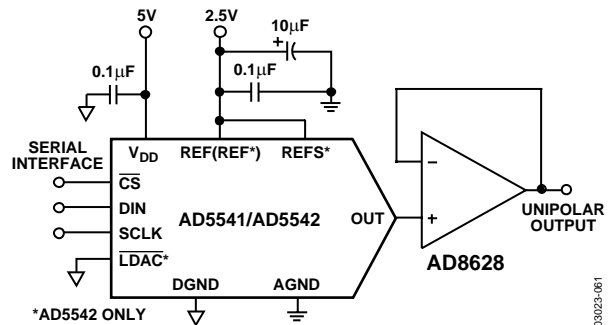
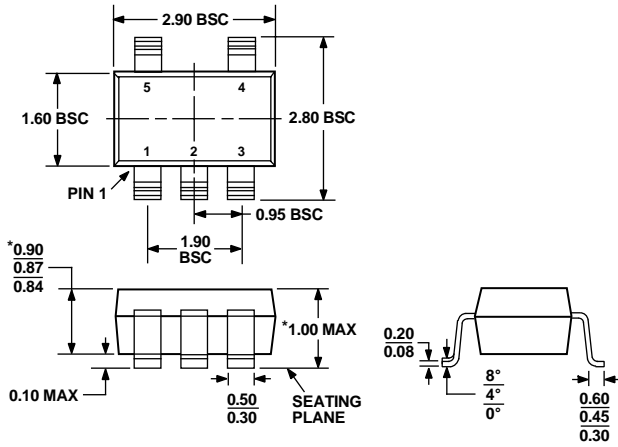


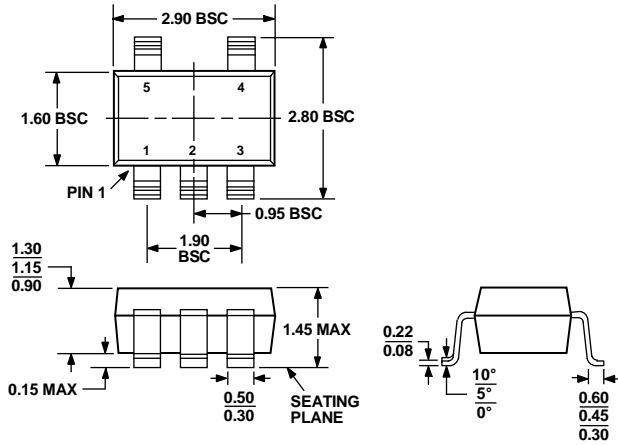
Figure 66. AD8628 Used as an Output Amplifier

OUTLINE DIMENSIONS



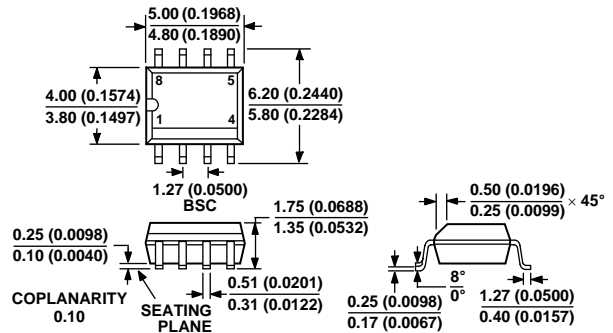
*COMPLIANT TO JEDEC STANDARDS MO-193-AB WITH THE EXCEPTION OF PACKAGE HEIGHT AND THICKNESS.

Figure 67. 5-Lead Thin Small Outline Transistor Package [TSOT] (UJ-5)
Dimensions shown in millimeters



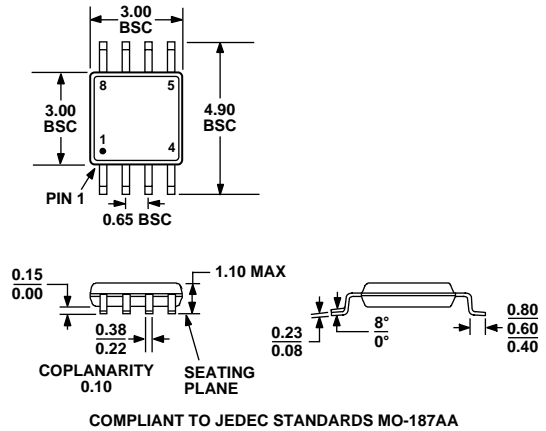
COMPLIANT TO JEDEC STANDARDS MO-178AA

Figure 68. 5-Lead Small Outline Transistor Package [SOT-23] (RT-5)
Dimensions shown in millimeters



COMPLIANT TO JEDEC STANDARDS MS-012AA
CONTROLLING DIMENSIONS ARE IN MILLIMETERS; INCH DIMENSIONS (IN PARENTHESES) ARE ROUNDED-OFF MILLIMETER EQUIVALENTS FOR REFERENCE ONLY AND ARE NOT APPROPRIATE FOR USE IN DESIGN

Figure 69. 8-Lead Standard Small Outline Package [SOIC] Narrow Body (R-8)
Dimensions shown in millimeters and (inches)



COMPLIANT TO JEDEC STANDARDS MO-187AA

Figure 70. 8-Lead Mini Small Outline Package [MSOP] (RM-8)
Dimensions shown in millimeters

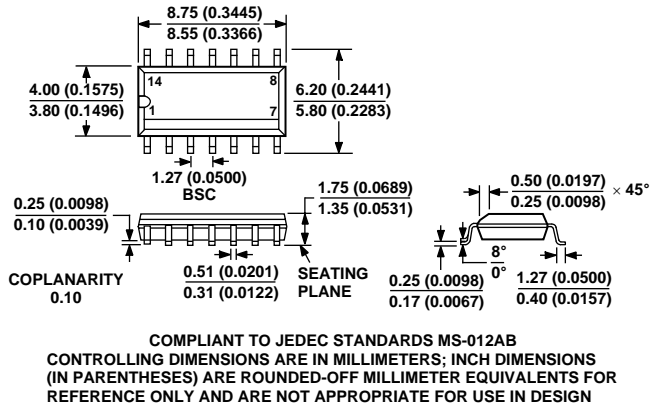


Figure 71. 14-Lead Standard Small Outline Package [SOIC]
Narrow Body
(R-14)
Dimensions shown in millimeters and (inches)

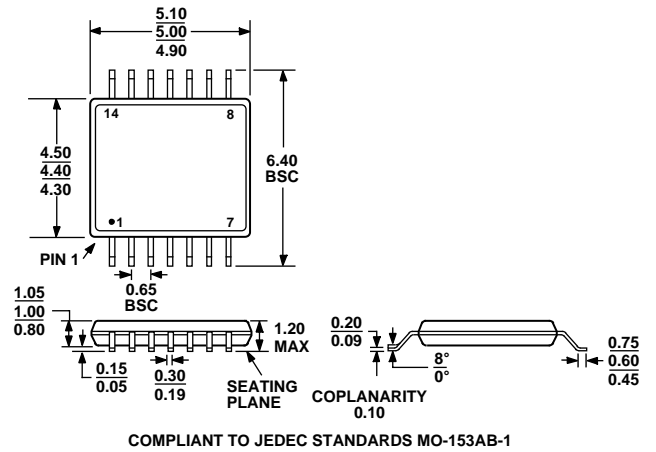


Figure 72. 14-Lead Thin Shrink Small Outline Package [TSSOP]
(RU-14)
Dimensions shown in millimeters

AD8628/AD8629/AD8630

ORDERING GUIDE

| Model | Temperature Range | Package Description | Package Option | Branding |
|-------------------------------|-------------------|---------------------|----------------|----------|
| AD8628AUJ-R2 | -40°C to +125°C | 5-Lead TSOT-23 | UJ-5 | AYB |
| AD8628AUJ-REEL | -40°C to +125°C | 5-Lead TSOT-23 | UJ-5 | AYB |
| AD8628AUJ-REEL7 | -40°C to +125°C | 5-Lead TSOT-23 | UJ-5 | AYB |
| AD8628AUJZ-R2 ¹ | -40°C to +125°C | 5-Lead TSOT-23 | UJ-5 | A0L |
| AD8628AUJZ-REEL ¹ | -40°C to +125°C | 5-Lead TSOT-23 | UJ-5 | A0L |
| AD8628AUJZ-REEL7 ¹ | -40°C to +125°C | 5-Lead TSOT-23 | UJ-5 | A0L |
| AD8628AR | -40°C to +125°C | 8-Lead SOIC | R-8 | |
| AD8628AR-REEL | -40°C to +125°C | 8-Lead SOIC | R-8 | |
| AD8628AR-REEL7 | -40°C to +125°C | 8-Lead SOIC | R-8 | |
| AD8628ARZ ¹ | -40°C to +125°C | 8-Lead SOIC | R-8 | |
| AD8628ARZ-REEL ¹ | -40°C to +125°C | 8-Lead SOIC | R-8 | |
| AD8628ARZ-REEL7 ¹ | -40°C to +125°C | 8-Lead SOIC | R-8 | |
| AD8628ART-R2 | -40°C to +125°C | 5-Lead SOT-23 | RT-5 | AYA |
| AD8628ART-REEL7 | -40°C to +125°C | 5-Lead SOT-23 | RT-5 | AYA |
| AD8628ARTZ-R2 ¹ | -40°C to +125°C | 5-Lead SOT-23 | RT-5 | A0L |
| AD8628ARTZ-REEL7 ¹ | -40°C to +125°C | 5-Lead SOT-23 | RT-5 | A0L |
| AD8629ARZ ¹ | -40°C to +125°C | 8-Lead SOIC | R-8 | |
| AD8629ARZ-REEL ¹ | -40°C to +125°C | 8-Lead SOIC | R-8 | |
| AD8629ARZ-REEL7 ¹ | -40°C to +125°C | 8-Lead SOIC | R-8 | |
| AD8629ARMZ-R2 ¹ | -40°C to +125°C | 8-Lead MSOP | RM-8 | A06 |
| AD8629ARMZ-REEL ¹ | -40°C to +125°C | 8-Lead MSOP | RM-8 | A06 |
| AD8630ARUZ ¹ | -40°C to +125°C | 14-Lead TSSOP | RU-14 | |
| AD8630ARUZ-REEL ¹ | -40°C to +125°C | 14-Lead TSSOP | RU-14 | |
| AD8630ARZ ¹ | -40°C to +125°C | 14-Lead TSSOP | R-14 | |
| AD8630ARZ-REEL ¹ | -40°C to +125°C | 14-Lead TSSOP | R-14 | |
| AD8630ARZ-REEL7 ¹ | -40°C to +125°C | 14-Lead TSSOP | R-14 | |

¹ Z = Pb-free part.

NOTES

AD8628/AD8629/AD8630

NOTES